Efficient, Mg^{2+}-Dependent Photochemical DNA Cleavage by the Antitumor Quinobenzoxazine (*S*)-A-62176†

Hongtao Yu,‡ Yan Kwok,§ Laurence H. Hurley,|| and Sean Michael Kerwin*

Division of Medicinal Chemistry and Institute for Cellular and Molecular Biology, The University of Texas at Austin, Austin, Texas 78712

Received May 16, 2000; Revised Manuscript Received June 23, 2000

ABSTRACT: The quinobenzoxazines, a group of structural analogues of the antibacterial fluoroquinolones, are topoisomerase II inhibitors that have demonstrated promising anticancer activity in mice. It has been proposed that the quinobenzoxazines form a 2:2 drug-Mg^{2+} self-assembly complex on DNA. The quinobenzoxazine (*S*)-A-62176 is photochemically unstable and undergoes a DNA-accelerated photochemical reaction to afford a highly fluorescent photoproduct. Here we report that the irradiation of both supercoiled DNA and DNA oligonucleotides in the presence of (*S*)-A-62176 results in photochemical cleavage of the DNA. The (*S*)-A-62176-mediated DNA photocleavage reaction requires Mg^{2+}. Photochemical cleavage of supercoiled DNA by (*S*)-A-62176 is much more efficient that the DNA photocleavage reactions of the fluoroquinolones norfloxacin, ciprofloxacin, and enoxacin. The photocleavage of supercoiled DNA by (*S*)-A-62176 is unaffected by the presence of SOD, catalase, or other reactive oxygen scavengers, but is inhibited by deoxygenation. The photochemical cleavage of supercoiled DNA is also inhibited by 1 mM KI. Photochemical cleavage of DNA oligonucleotides by (*S*)-A-62176 occurs most extensively at DNA sites bound by drug, as determined by DNase I footprinting, and especially at certain G and T residues. The nature of the DNA photoproducts, and inhibition studies, indicate that the photocleavage reaction occurs by a free radical mechanism initiated by abstraction of the 4′- and 1′-hydrogens from the DNA minor groove. These results lend further support for the proposed DNA binding model for the quinobenzoxazine 2:2 drug-Mg^{2+} complex and serve to define the position of this complex on the minor groove of DNA.

The synthetic quinobenzoxazines are a new class of antineoplastic agents (*1*, *2*). Although they are structural analogues of the antibacterial fluoroquinolones such as norfloxacin and ciprofloxacin, these two classes of compounds have distinct biological activities. While the quinobenzoxazines display in vitro and in vivo anticancer activity (*2*, *3*) and are mammalian (*4*, *5*) topoisomerase II inhibitors, the typical fluoroquinolones have no antitumor activity and are normally bacterial topoisomerase II (gyrase) or topoisomerase IV inhibitors (*6*−*10*). The extended planar tetracyclic chromophore of the quinobenzoxazines enables them to intercalate into duplex DNA (*11*), while fluoroquinolones with the fused bicyclic ring system prefer to bind to single-stranded DNA or to a duplex DNA−gyrase complex (*12*−*14*). The intercalation complex of the quinobenzoxazines with duplex DNA has been proposed to involve a drug dimer linked by two Mg^{2+} ions. This drug-Mg^{2+} dimer is readily formed in solution, even from micromolar concentrations of drug, in the presence of Mg^{2+} (*15*) with one drug molecule intercalated into DNA base pairs and the second drug molecule externally bound through the interactions with the DNA groove (*11*).

The quinobenzoxazines are photosensitive in neutral aqueous solutions. Irradiation (>300 nm) of quinobenzoxazine solutions produces photoproducts, one of which is strongly fluorescent with an emission peak at 442 nm (*15*). This photoreaction is greatly accelerated in the presence of DNA and Mg^{2+} due to the formation of the specific drug−Mg^{2+} intercalation complex with DNA. The photoreaction is proposed to be initiated by electron transfer from a quinobenzoxazine molecule in its photoexcited state to an electron acceptor. The drug radicals thus formed can react with available chemical species in the solution, such as solvent, cellular components such as DNA, or even parent drug molecules, to form photoproducts (*15*). Due to the possible DNA damage by drug radicals, these antibacterial/anticancer agents may be phototoxic. In fact, many fluoroquinolones have been found to be phototoxic (*16*−*19*), and this phototoxicity may be related to photochemical DNA damage (*20*−*24*). Therefore, the phototoxicity should be avoided for future development of this type of antibacterial/anticancer drugs. On the other hand, the photoreactivity of the quinobenzoxazines or fluoroquinolones can be a useful tool to study their interactions with the DNA-topoisomerase II or DNA−gyrase complex (*5*).

† This work was supported by the United States Public Health Service Grants GM-50892 (to S.M.K.) and CA-49751 (to L.H.H.).

* To whom correspondence should be addressed: Phone: (512) 471-5074. Fax: (512) 232-2606. E-mail: skerwin@mail.utexas.edu.

‡ Current address: Department of Chemistry, Jackson State University, Jackson, MS 39217.

§ Current address: Genelabs Technologies, Inc., 505 Penobscot Drive, Redwood City, CA 94063.

|| Current address, Arizona Cancer Center, University of Arizona, 1515 N. Cambell Ave., Tucson, AZ 85724.

10.1021/bi001103x CCC: $19.00
Published on Web 07/26/2000

Chart 1

77-mer DNA

(+) 5′CGCAGCGCGCGATTGAAGCGGCGCACGAAAAACGCGAAAGCGTTTCACGATAAATGCGAAAACTTGCAACGCGCTGT 3′

(−) 3′ TCGCGCGCTAACTTCGCCGCGTGCTTTTTGCGCTTTCGCAAAGTGCTATTTACGCTTTTGAACGTTGCGCGACAGCG 5′

In this paper, we present a study of the photosensitized DNA damage to both phage DNA and DNA oligonucleotides due to the quinobenzoxazine (*S*)-A-62176, (*S*)-1-(3-aminopyrrolidin-1-yl)-2-fluoro-4-oxo-4H-quino[2,3,4-ij][1,4]-benzoxazine-5-carboxylic acid. The photodamage to DNA by (*S*)-A-62176 produces multiple types of products including frank strand breakage products and a base-labile product. Through studies of agents that quench the fluorescence of DNA-bound (*S*)-A-62176, the photocleavage of DNA by (*S*)-A-62176, and the DNA-facilitated photoreaction of (*S*)-A-62176, a free radical DNA cleavage mechanism is proposed. The DNA photocleavage by (*S*)-A-62176 provides further evidence for and refinements in the previously proposed dimeric intercalation DNA binding model for this class of compounds.

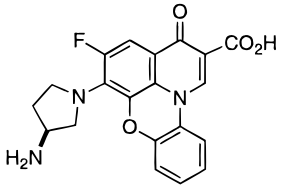

(*S*)-A62176

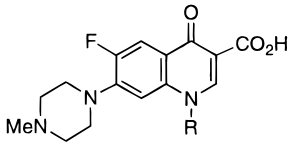

Norfloxacin R = ethyl
Ciprofloxacin R = cyclopropyl

MATERIALS AND METHODS

Materials, Enzymes, and Drugs. The quinobenzoxazine (*S*)-A-62176 and its racemic 5-descarboxy derivative (dC-A-62176) were kindly provided by Abbott Laboratories (*1*, *2*). Bleomycin was a gift from Dr. Daekyu Sun (Institute for Drug Development, San Antonio, TX). Norfloxacin, ciprofloxacin, and enoxacin; ΦX-174 phage DNA, SOD,[1] catalase, and ferrous ammonium sulfate were purchased from Sigma. EDTA and MB were from Fisher Scientific. $NaBH_4$, $MgCl_2$ (99.99%), 2-propanol, glycerol, DMSO, TMP, thiourea, DTT, and NaN_3 were from Aldrich. Electrophoretic reagents (acrylamide, *N*,*N*′-methylenebisacrylamide, ammonium persulfate) were from J. T. Baker, Inc. T4 polynucleotide kinase, Klenow fragment of DNA polymerase I, DNase I and [γ-^{32}P]ATP were from Amersham.

Preparation and End-Labeling of Oligonucleotides. The 15-mer, 18-mer, 26-mer, and 77-mer DNA (Chart 1) were synthesized on an Applied Biosystems 381A DNA synthesizer using standard phosphoramidite chemistry. The oligonucleotides were cleaved from the column material by concentrated ammonium hydroxide (Fisher) and the resulting solution was heated overnight at 55 °C to afford deprotected material. The single-stranded DNA fragments were purified by electrophoresis on a 12% preparative denaturing polyacrylamide gel.

The 5′-end-labeled single-stranded oligonucleotides were obtained by incubating the oligonucleotides with T4 polynucleotide kinase and [γ-^{32}P]ATP. The labeled single strands were annealed with their unlabeled complementary strands to make the (+) or (−) strand end-labeled duplex DNA, which were then purified by electrophoresis on an 8% native polyacrylamide gel.

The 3′-end-labeled 18-mer DNA was obtained by enzymatic extension of the 3′-end of the 15−18 mer DNA (Chart 1) with the Klenow fragment of DNA polymerase I and [α-^{32}P]dATP and cold dCTP. The labeled DNA was separated from unincorporated [α-^{32}P]dATP by electrophoresis on a native 20% polyacrylamide gel.

26-mer DNA

5′GAAAGCGTTTCACGATAAATGCGAAA 3′

3′CTTTCGCAAAGTGCTATTTACGCTTT 5′

18-mer DNA

5′CAGGCTTTGCGATCGCCA 3′

3′GTCCGAAACGCTAGCGGT 5′

15−18-mer DNA for 3′-end labeling

5′CAGGCTTTGCGATCG 3′

3′GTCCGAAACGCTAGCGGT 5′

Photocleavage of ΦX-174 phage DNA. ΦX-174 phage DNA (80 μM in base pairs) was incubated with various amounts of drug in 60 μL of a buffer containing 2 mM $MgCl_2$ and 20 mM sodium phosphate (pH 7.5), in the presence of free radical/singlet oxygen scavengers: NaN_3 (0.1−10 mM), DTT (0.1−10 mM), DMSO (0.1−0.5 M), TMP (0.1−0.5 M), 2-propanol (0.1−0.5 M), ethylene glycol (0.1−0.5 M); fluorescence quencher KI (1 or 10 mM); or enzymes: SOD (25 μg/mL) and catalase (25 μg/mL). The samples were loaded onto a 24-well Titertek microtiter plate (ICN) and either allowed to stand at room temperature under ambient light or placed on top of a Pyrex glass shield and irradiated with an 85 W Xe lamp (George W. Gates, Inc.). The lamp was placed 12 cm directly underneath the Pyrex glass filter, which served to eliminate DNA damage caused directly by UV irradiation. A stream of cool air blowing on the bottom of the Pyrex glass prevented heating of the sample during the irradiation. During the irradiation, the Titertek plate was rotated every 15 min to average the effects of the light inheterogeneity. Samples were irradiated for various times, then placed in the dark before loading onto an agarose gel. After irradiation, 8 μL of loading dye (0.25% bromophenol blue, 0.25% xylene cyanol and 25 mM EDTA in 50% glycerol) was added to each sample, and each sample was loaded onto a 0.8% agarose gel containing ethidium bromide (0.5 μg/mL). After electrophoresis at 90 V for approximately 3 h, the DNA was visualized by UV light and photographed

[1] Abbreviations: DMSO, dimethyl sulfoxide; DTT, dithiothreitol; EDTA, *N*,*N*,*N*′,*N*′-ethylenediaminetetraacetic acid; HEPES, *N*-(2-hydroxyethyl)piperazine-*N*′-(2′-ethanesulfonic acid); MB, methylene blue; SOD, superoxide dismutase; TMP, 2,2,5,5-tetramethylpiperidine.

with Polaroid 667 film. Quantification of the three forms of DNA, supercoiled (form I), linear (form III), and nicked circular (form II) was done by densitometric scanning of the film negative and corrected for the decreased binding of ethidium bromide to supercoiled DNA (70% staining efficiency, assuming 100% staining efficiency for both the relaxed and linear DNA) (25).

Quenching of the Fluorescence and Photoreaction of (S)-A-62176 by Various Reagents. Fluorescence emission intensities at 500 nm (380 nm_{ex}) of a 5 μM solution of (*S*)-A-62176 (2 mM $MgCl_2$, 20 mM sodium phosphate, pH 7.5) in the presence of 80 μM calf thymus DNA were measured at various concentrations of added fluorescence quenching agents. The concentration of each quenching agent necessary to cause a 50% decrease in the intensity of the fluorescence emission by (*S*)-A-62176 (C_{50}^{F}) was obtained from plots of the fluorescence intensity versus quencher concentrations.

The inhibition of the photodegradation of (*S*)-A-62176 by these reagents was also determined. Solutions (80 μL total volume in 20 mM sodium phosphate at pH 7.5) of 5 μM (*S*)-A-62176 containing 80 μM calf thymus DNA and various concentrations of quenching agents were irradiated for 5 min in a quartz cuvette under argon with an 85 W xenon lamp as described above. After irradiation, the fluorescence emission intensity of the photoproduct ($F_{420/5min}$) was measured at 420 nm (380 nm_{ex}). This intensity is proportional to the amount of photoproduct formed (*15*). The concentration of the quenching agents necessary to cause a 50% decrease in the $F_{420/5min}$ (C_{50}^{R}) was obtained from the plot of the $F_{420/5min}$ versus quencher concentration. The $F_{420/5min}$ was corrected for the effect of (*S*)-A-62176 photoproduct fluorescence quenching by the added agents.

DNA Photocleavage under Air or Argon. A solution containing ΦX-174 DNA (80 μM in base pairs) and (*S*)-A-62176 (0.1 or 1 μM) in the presence of 2 mM $MgCl_2$ (80 μL total volume in 20 mM sodium phosphate, pH 7.5) was placed in a semimicro quartz cuvette (0.4 × 1 cm, Uvonic). The cuvette was sealed by a rubber septum fitted with a Teflon tube and a needle as gas inlet and outlet, respectively. The samples in the cuvette were purged with air or argon (Air Liquide) through the Teflon tube for 10 min before irradiation and continuously during the irradiation. The argon was deoxygenated by bubbling through a freshly prepared Fieser's solution [15 g of sodium dithionite ($Na_2S_2O_4$), 2 g of sodium anthraquinone-β-sulfonate, 20 g of KOH in 100 mL of water] followed by a saturated lead acetate solution. The cuvette was placed horizontally on top of a Pyrex glass filter, which was 12 cm above the Xe lamp. After irradiation, the samples were transferred to eppendorf tubes and stored in the dark at 4 °C before the addition of loading dye and agarose gel electrophoresis as described above.

Photocleavage of Synthetic Oligonucleotides by (S)-A-62176. The end-labeled duplex DNA (0.2−3 μM in base pairs) was incubated with various concentrations of (*S*)-A-62176 in 60 μL of a buffer containing 20 mM sodium phosphate (pH 7.5) with or without 2 mM $MgCl_2$. The samples were loaded onto a 24-well Titertek microtiter plate on top of a Pyrex glass shield placed 9 cm above a 85 W Xe lamp and irradiated for 2 h as described above. The reactions were terminated by adding 10 μg of calf thymus DNA. To determine the effects of alkaline and reductive conditions on the nature of the photocleavage products, the sample from one single photocleavage reaction was divided into 4 aliquots: one aliquot was subjected to ethanol precipitation; the other three aliquots were treated with $NaBH_4$, piperidine, and NaOH, respectively. (1) $NaBH_4$: a solution of $NaBH_4$ (1 M, freshly prepared in water) was added in three equal portions at 30-min intervals to a final concentration of 0.3 M. Excess $NaBH_4$ was destroyed by glacial acetic acid as described previously (*26*), followed by ethanol precipitation. (2) Piperidine: the aliquot was heated at 95 °C with 0.1 M piperidine for 20 min before ethanol precipitation. (3) NaOH: the aliquot was heated with 0.1 M NaOH at 90 °C for 3 min before ethanol precipitation.

DNA Cleavage by Bleomycin. The 5′-end-labeled duplex DNA (5 μM in base pairs) in 40 μL of a buffer containing 50 mM HEPES (pH 7.5), 100 mM NaCl, and 0.48 μg/μL calf thymus DNA was incubated with 40 μL of 500 μM of activated bleomycin at 4 °C for 10 min, followed by ethanol precipitation. Activated bleomycin was prepared by mixing equal volumes of 1 mM bleomycin in 5 mM HEPES (pH 7.5) and 1 mM ferrous ammonium sulfate at 4 °C for 1 min.

DNase I Digestion of the 77-mer DNA in the Presence of (S)-A-62176. The 5′-end-labeled 77-mer DNA (0.2 μM in base pairs) was mixed with various amounts of (*S*)-A-62176 for 10 min at room temperature in 20 μL of a solution containing 20 mM sodium phosphate (pH 7.5) and 2 mM $MgCl_2$. Reaction mixtures to which 0.05 unit of DNase I was added were incubated for 1 min. The DNase I reaction was quenched by the addition of 180 μL of a solution containing 3 mM EDTA, 0.3 M sodium acetate, and 5 μg of tRNA, followed by ethanol precipitation.

Hydroxyl Radical Cleavage of the 26-mer DNA. Ferrous ammonium sulfate (2 μL of 0.375 mM), EDTA (2 μL of 0.75 mM), sodium ascorbate (2 μL of 15 mM) and H_2O_2 (2 μL of 7.5%) were added to a solution (24 μL) containing the 5′-end-labeled 26-mer or 18-mer DNA (0.1 μM in base pairs) in a buffer of 20 mM sodium phosphate (pH 7.5) and 2 mM $MgCl_2$. The reaction mixture was incubated at room temperature for 5 min and the reaction was quenched by addition of 170 μL of solution containing 10 μL of 1 M thiourea, 20 μL of 3 M sodium acetate and 10 μg of tRNA, followed by ethanol precipitation.

Sequencing Gel Electrophoresis. The labeled, dried DNA pellets were dissolved in alkaline dye (80% formamide and 10 mM NaOH, 1 mM EDTA, 0.1% xylene cyanol, and 0.1% bromophenol blue) and loaded onto either a 20% (18-mer), 16% (26-mer) or a 12% (77-mer) sequencing polyacrylamide gel. Gels were subjected to electrophoresis at 1800−2200 V and 30 mA for approximately 3 h. The dried gels were autoradiographed on X-ray films, which were scanned by an Epson Scanner model ES-1200. The quantification was performed by ImageQuaNT 4.1 software from Molecular Dynamics.

RESULTS

Photochemical Single-Strand DNA Cleavage by (S)-A-62176 Requires Mg^{2+}. The quinobenzoxazine (*S*)-A-62176 is a very efficient DNA photocleavage agent. When supercoiled (form I) ΦX-174 phage DNA (80 μM base pairs, 82% form I) is incubated with (*S*)-A-62176 (2.5 μM) in the presence of 2 mM $MgCl_2$ under ambient light conditions,

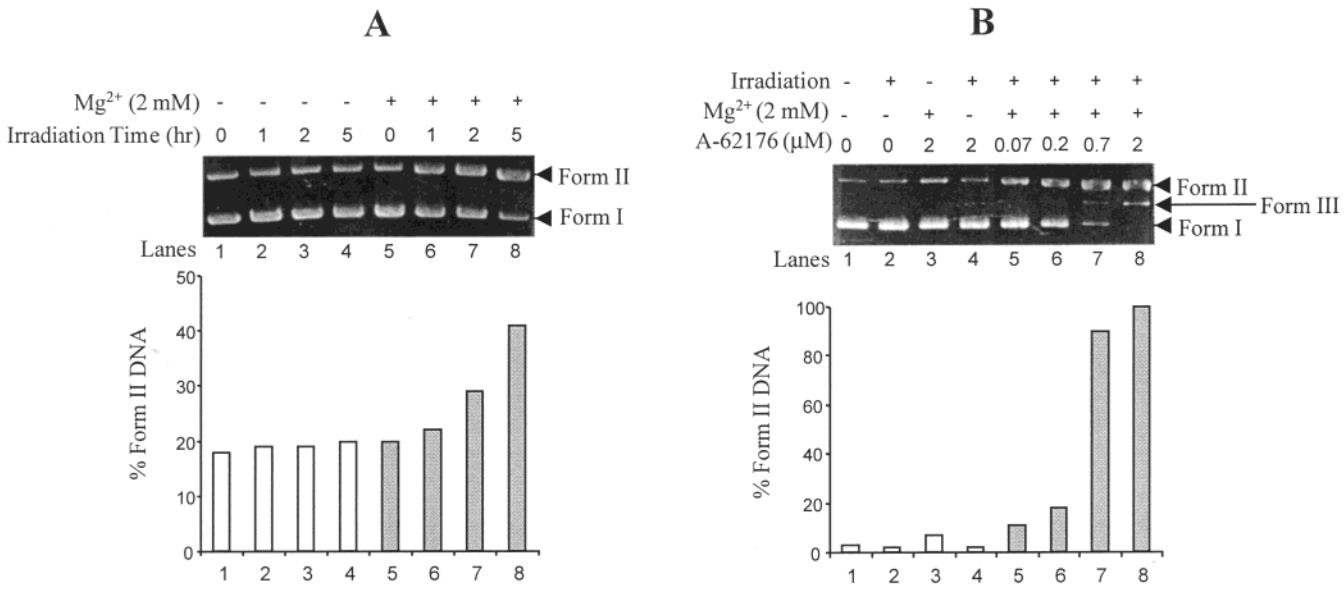

FIGURE 1: Photocleavage of ΦX-174 phage DNA by (*S*)-A-62176 under ambient light (A) or an 85W xenon lamp (B). Forms I, II, and III represent supercoiled, open circular, and linear DNA, respectively. Top panels of A and B show the photographs of the 0.8% agarose gel. Bottom panels of A and B show the densitometric analysis of the form II products detected in the agarose gels above. Lanes 1−8 in panel A contain 2.5 μM of (*S*)-A-62176. The irradiation time in panel B was 30 min.

the supercoiled DNA is converted to circular relaxed (form II) DNA (Figure 1A, lanes 5−8). In the absence of added $MgCl_2$, no DNA cleavage is detected (lanes 1−4). The amount of form I DNA converted to form II DNA is proportional to the length of irradiation by ambient light (see Figure 1A bottom); after 8 h of irradiation only 58% of form I DNA remains (~30% cleavage). No linear (form III) DNA is produced under these conditions, indicating that the Mg^{2+}-dependent DNA photocleavage due to (*S*)-A-62176 involves only single-strand DNA cleavage.

If an 85 W xenon lamp is used as a light source in place of ambient light, the photocleavage of supercoiled DNA by (*S*)-A-62176 is much more extensive. After 30 min of irradiation in the presence of 2 μM (*S*)-A62176 and 2 mM $MgCl_2$, all form I ΦX-174 DNA is consumed, producing form II and a small amount of linear form III DNA (Figure 1B, lane 8). The photocleavage of DNA is a function of the concentration of (*S*)-A-62176 (see lanes 5−8 in Figure 1B); significant photocleavage is observed even at concentrations as low as 70 nM of (*S*)-A-62176 (lane 5). When irradiated under the Xe lamp in the absence of Mg^{2+} ions, (*S*)-A-62176 does not affect the photocleavage of supercoiled DNA (lane 4, Figure 1B). There is no cleavage observed when supercoiled DNA is incubated with (*S*)-A-62176 and $MgCl_2$ in the dark (lane 3, Figure 1B).

(S)-A-62176 Photocleaves DNA More Efficiently Than Its 5-Descarboxy Derivative, Methylene Blue, and the Antibacterial Fluoroquinolones. The ability of (*S*)-A-62176 to cause the photochemical cleavage of supercoiled DNA was compared with other DNA photocleavage agents and quinobenzoxazine analogues. A typical gel for the photocleavage of supercoiled phage DNA by selected antibacterial fluoroquinolones (norfloxacin, ciprofloxacin and enoxacin) in comparison with (*S*)-A-62176 is shown in Figure 2. Irradiation of ΦX-174 DNA (80 μM, 75% form I) for 30 min in the presence of 0.15 μM of (*S*)-A-62176 in Mg^{2+}-containing buffer is sufficient to convert nearly all of the form I DNA to form II (73% cleavage) (lane 3, Figure 2). In contrast,

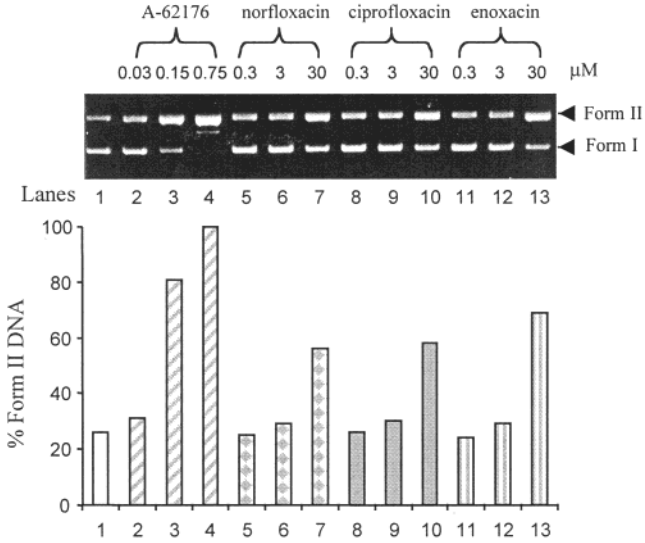

FIGURE 2: Photocleavage of ΦX-174 phage DNA in 20 mM sodium phosphate, 2 mM $MgCl_2$ buffer, pH 7.5, by (*S*)-A-62176, norfloxacin, ciprofloxacin, and enoxacin under the 85 W xenon lamp light. Lane 1 is control DNA without drug. The irradiation time was 45 min.

much higher concentrations of the antibacterial fluoroquinolones are required in order to effect the same level of DNA photocleavage as that observed with (*S*)-A-62176. Irradiation of supercoiled DNA in the presence of 30 μM norfloxacin (lane 7), ciprofloxacin (lanes 10), or enoxacin (lane 13) results in only 41, 44, and 59% DNA cleavage, respectively. The relative DNA photocleavage efficiency of these fluoroquinolones is therefore over 200-fold less than that of (*S*)-A-62176. Using the same analysis, the relative DNA photocleavage efficiency of these and other selected compounds when compared to (*S*)-A-62176 were determined and are shown graphically in Figure 3. Methylene blue (MB) converts supercoiled form I DNA to relaxed form II 50-times less efficiently than (*S*)-A-62176 under these reaction conditions (Figure 3). The 5-descarboxy derivative of (*S*)-A-62176

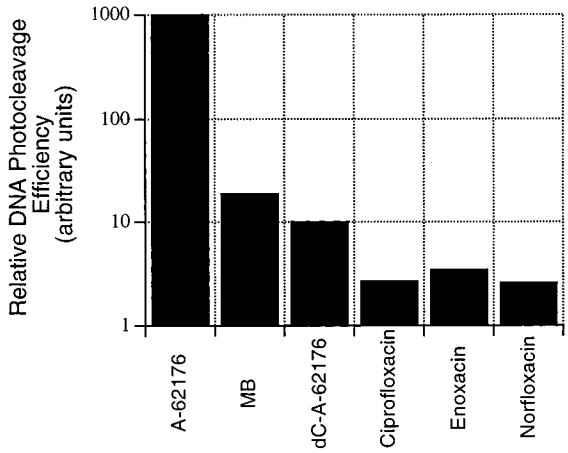

FIGURE 3: Relative efficiency of photochemical DNA cleavage by the quinobenzoxazines (*S*)-A-62176 and its descarboxy derivative (dC-A-62176), the fluoroquinolones norfloxacin, ciprofloxacin, and enoxacin, and methylene blue (MB). For each compound, the concentration required to effect 50% conversion of form I to form II DNA was estimated, divided by the concentration of (*S*)-A-62176 required, and multiplied by 1000.

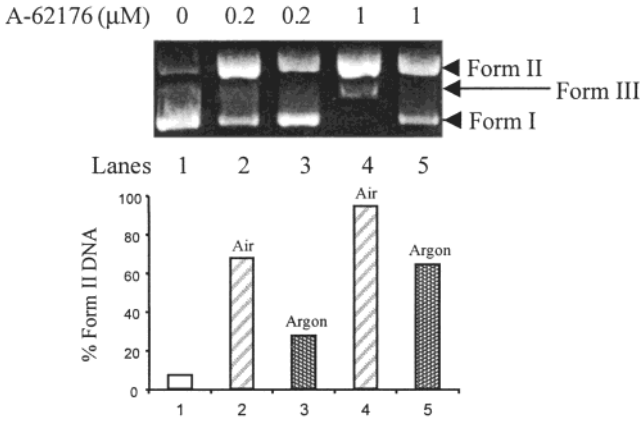

FIGURE 4: Photocleavage of ΦX-174 phage DNA by (*S*)-A-62176 under air or argon. The irradiation time was 45 min.

(dC-A-62176) is at least 100-times less efficient than (*S*)-A-62176 in converting form I to form II DNA (Figure 3). In all of the above cases, there was no evidence of double-stranded DNA photocleavage by any of these compounds; linear form III DNA was only observed after the majority of the form I DNA was converted into form II in samples that were irradiated for longer periods of time.

Photocleavage of DNA by (S)-A-62176 Is Unaffected by the Presence of SOD, Catalase, or Other Free Radical and Reactive Oxygen Scavengers, But Inhibited by Deoxygenation. The potential role of reactive oxygen species in the DNA photocleavage due to (*S*)-A-62176 was investigated. DNA photocleavage reaction mixtures were degassed by sparging with deoxygenated argon gas before and during irradiation. Figure 4 shows the photocleavage of ΦX-174 phage DNA in the presence of 0.2 and 1 μM (*S*)-A-62176 and 2 mM Mg^{2+} under these anaerobic conditions (lanes 3 and 5) or under air (lanes 2 and 4). Under anaerobic conditions, photochemical cleavage of DNA by 0.2 μM (*S*)-A-62176 is inhibited 57%, compared to photocleavage in air. At higher concentrations of quinobenzoxazine, the inhibition of DNA photocleavage due to deoxygenation is only 25%. The lower level of photocleavage observed under

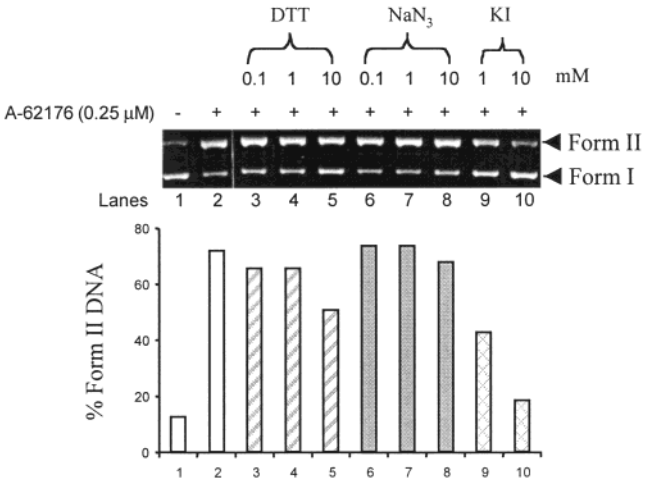

FIGURE 5: Photocleavage of ΦX-174 phage DNA by (*S*)-A-62176 in the presence of various concentrations of free radical scavengers. The irradiation time was 30 min.

argon may be due to either a second, oxygen-independent photocleavage pathway, or to traces of oxygen that remain even after the reaction mixtures are purged with argon.

To determine if hydroxyl radicals or superoxide are produced during photochemical DNA cleavage, the photocleavage reactions were carried out in the presence of scavengers of these intermediates. The photocleavage of supercoiled phage DNA by (*S*)-A-62176 in the presence 25 μg/mL of SOD, which converts superoxide to hydrogen peroxide, or catalase, which converts hydrogen peroxide to water and oxygen, is as efficient as when these scavengers are absent (data not shown). These results indicate that superoxide and hydrogen peroxide are not involved DNA cleavage.

The effects of other free radical and singlet oxygen scavengers on the photocleavage of DNA by (*S*)-A-62176 were also determined. Singlet oxygen scavenger TMP and free radical scavengers 2-propanol, glycerol, and DMSO at concentrations of up to 0.5 M have no detectable effects on the photocleavage of ΦX-174 phage DNA by (*S*)-A-62176 (data not shown). Very weak inhibition of photochemical DNA cleavage is observed with added DTT (lanes 3−5, Figure 5) and NaN_3 (lanes 6−8). The amount of relaxed DNA formed after 45 min of irradiation in the presence of 0.25 μM (*S*)-A-62176 is reduced by only 30% and 10% in the presence of 10 mM of DTT (lane 5) or NaN_3 (lane 8), respectively. At lower concentrations, DTT and NaN_3 have no effect on the DNA photocleavage due to (*S*)-A-62176. These results indicate that a diffusable free-radical species is probably not involved in the photochemical DNA cleavage.

Quenching of the Fluorescence of DNA-Bound (S)-A-62176 and Inhibition of the DNA-Facilitated Photodecomposition of (S)-A-62176 by KI and DTT. To understand whether the photocleavage of DNA induced by (*S*)-A-62176 originates from the singlet excited state of (*S*)-A-62176, we investigated the ability of certain agents to quench the fluorescence of the complex formed between (*S*)-A-62176, Mg^{2+}, and double-stranded DNA. The fluorescence intensity of solutions containing 5 μM (*S*)-A-62176, 2 mM $MgCl_2$, and 80 μM calf thymus DNA in 20 mM phosphate buffer was determined as a function of the amount of added quenching agent, and the concentration of quenching agent

Table 1: (*S*)-A-62176 Fluorescence Quenching and DNA-Facilitated (*S*)-A-62176 Photoreaction Inhibition

	C_{50}^{F} (*S*)-A-62176 fluorescence quenching (mM)[a]	C_{50}^{R} (*S*)-A-62176 photoreaction inhibition (mM)[b]
DTT	600	0.05[c]
NaN3	*d*	4[e]
KI	45	0.15[f]
thiourea	*d*	10[g]

[a] Concentration (mM) necessary to halve the 500 nm fluorescence of the (*S*)-A-62175-Mg^{2+}-DNA complex. [b] Concentration (mM) necessary to halve the amount of 420 nm fluorescent photoproduct formed from the (*S*)-A-62176-Mg^{2+}-DNA complex after irradition for 5 min. [c] The C_{50}^{F} for the photoproduct is 100 mM. [d] Too high to be measured. [e] The C_{50}^{F} for the photoproduct is 22 mM. [f] The C_{50}^{F} for the photoproduct is 30 mM. [g] The C_{50}^{F} for the photoproduct is 20 mM.

necessary to decrease the fluorescence due to the quinobenzoxazine−DNA complex by half (C_{50}^{F}) was determined (Table 1). NaN_3 and thiourea have no measurable effect on the fluorescence of the DNA-bound (*S*)-A-62176 (Table 1); these compounds do not quench the excited singlet state of the DNA-bound (*S*)-A-62176. In contrast, both DTT and KI were found to quench the fluorescence of the quinobenzoxazine−DNA complex. The quenching of the fluorescence of the quinobenzoxazine−DNA complex by DTT is somewhat less efficient than that due to KI.

Independent of their ability to quench the fluorescence of the DNA-bound quinobenzoxazine−Mg^{2+} complex, these compounds display widely different abilities to inhibit the DNA-facilitated photodecomposition of (*S*)-A-62176. Solutions containing 5 μM (*S*)-A-62176, 2 mM $MgCl_2$, 80 μM calf thymus DNA, and various concentrations of quenching agents in 20 mM phosphate were irradiated for 5 min under an 85W xenon lamp, and the fluorescence intensity at 420 nm, due to the quinobenzoxazine photoproduct, was determined. The concentration of inhibitor necessary to half the 420 nm fluorescence in the photoreaction (C_{50}^{R}) was determined. Control experiments involving addition of quenching agents after the irradiation established the ability of these same compounds to quench the fluorescence of the photoproduct. DTT is the most efficient inhibitor of the DNA-facilitated photodecomposition of (*S*)-A-62176. The C_{50}^{R}, for DTT is significantly less than either the concentration necessary to quench the fluorescence of the DNA-bound quinobenzoxazine (C_{50}^{F} = 600 mM) or the photoproduct fluorescence (100 mM). Although not as effective as an inhibitor of the photodecomposition of (*S*)-A-62176, KI also inhibits the production of the fluorescent photoproduct at a concentration (150 μM) that is significantly less than that required to quench the fluorescence of the DNA-bound quinobenzoxazine (45 mM) or of the photoproduct (30 mM). In contrast, both NaN_3 and thiourea are far less effective in inhibiting the photodecomposition of (*S*)-A-62176, and the concentrations required are close to those found to quench the photoproduct fluorescence, indicating that they may be even poorer inhibitors than their C_{50}^{R} values (4 and 10 mM, respectively) would indicate.

Photocleavage of ΦX-174 Phage DNA by (S)-A-62176 Is Inhibited in the Presence of KI. The amount of form II DNA induced by 0.25 μM (*S*)-A-62176 after 30 min of irradiation is inhibited by increasing concentrations of added KI (Figure 5, lanes 9 and 10). The photocleavage due to (*S*)-A-62176 (lane 2) is almost completely abolished in the presence of 10 mM KI (lane 10), and at 1 mM concentration of KI, approximately one-half of the photocleavage observed in its absence is produced. The degree of inhibition of the quinobenzoxazine photocleavage reaction by KI is significantly more than that observed with DTT and NaN_3. The concentration of KI required to inhibit the photocleavage reaction is significantly higher than the C_{50}^{R}, indicating that the production of this fluorescent photoproduct is not required for photochemical DNA cleavage. In contrast, the concentration of KI required to inhibit the photochemical DNA cleavage reaction is less than the C_{50}^{F} for KI, indicating that the inhibition of photochemical DNA cleavage by KI is not due to singlet quenching of the photoexcited quinobenzoxazine.

Irradiation of DNA in the Presence of (S)-A-62176 and Mg^{2+} Produces a Complex Pattern of Frank Strand Breaks, as Revealed by Gel Electrophoresis. To analyze the sequence selectivity and the nature of the DNA termini resulting from the photocleavage reaction, 5′- and 3′-end-labeled oligonucleotides were subjected to photocleavage in the presence of (*S*)-A-62176, and the reaction products analyzed by gel electrophoresis. The gel electrophoretic pattern of a 5′-end labeled 26-mer oligonucleotide (Chart 1) following irradiation in the presence of (*S*)-A-62176 and Mg^{2+} is shown in Figure 6, panels A and B. The concentration dependent photochemical strand breakage is shown in lanes 6−11 in both panels A and B (in panel B, heat-piperidine treatment of the DNA was performed after the irradiation). In contrast to the photocleavage of phage ΦX-174 DNA, in which the ratio of (*S*)-A-62176 to DNA base-pairs was much less than unity, in the oligonucleotide photocleavage experiments, optimal photocleavage of the 26-mer is observed at 0.5 μM of (*S*)-A-62176 (lane 8). At this concentration the drug:DNA (base pair) ratio is 2:1, and no further increase in the efficiency of DNA photocleavage is observed at higher (*S*)-A-62176 concentrations. Control experiments (lanes 1−4) demonstrate that oligonucleotide DNA strand cleavage requires the presence of (*S*)-A-62176, Mg^{2+}, and irradiation, as was observed for phage DNA photocleavage.

The 5′-end labeled oligonucleotide DNA photocleavage products afford, upon gel electrophoresis, a pair of bands of nearly equal intensity at each cleaved DNA site (Figure 6, panels A and C). These two bands represent (at least) two DNA frank strand cleavage products at each DNA base site. Comparison of the mobilities of these two bands with those in the Maxam-Gibert sequencing lanes (lanes AG and TC) and hydroxyl radical cleavage lane (lane 12) reveals that the slower moving band of each doublet comigrates with the Maxam-Gibert sequencing reaction and hydroxyl radical cleavage products (Figure 6C), which are known to be the 3′-phosphates (*27*, *28*). On the other hand, the faster moving band of each doublet appears to comigrate with the minor products of the hydroxyl radical cleavage reaction (Figure 6C), which are 3′-phosphoglycolic acids (*28*). Treatment of the cleavage products with $NaBH_4$ does not alter the mobilities of the faster moving bands in each doublet (lane 6, Figure 7), indicating the absence of 3′-phosphoglyceraldehyde termini products, which would have been reduced to the faster migrating 3′-phosphoglycol termini products

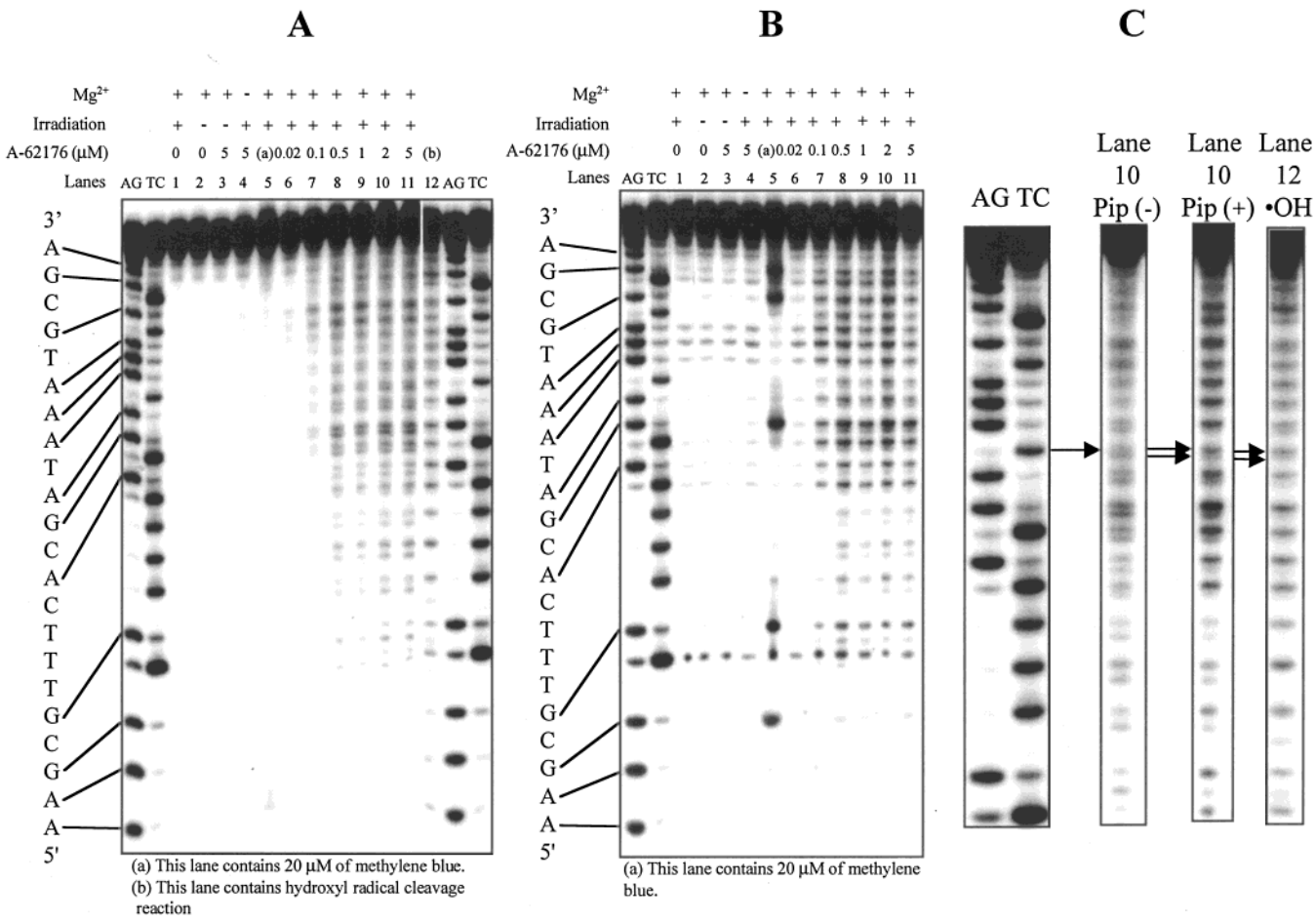

FIGURE 6: Photocleavage of the 5′-end labeled 26-mer DNA (0.2 μM in base pairs) by (*S*)-A-62176. (A, B, and C) Autoradiogram of 16% denaturing polyacrylamide gels showing the DNA cleavage patterns. Lanes AG and TC contain the Maxam−Gilbert sequencing reactions. Lane 5 contains 20 μM of methylene blue and lane 12 contains the hydroxyl radical cleavage reaction. (A) Before piperidine treatment. (B) After piperidine treatment. (C) Direct comparisons of the products from Maxam−Gilbert sequencing (lane AG and TC) and hydroxyl radical cleavage (lane 12) reactions with the photocleavage product of DNA by 2 μM of (*S*)-A-62176 before piperidine (lane 10 of panel A) and after piperidine treatment (lane 10 of panel B).

(*29*). Furthermore, the faster moving band of these doublets from the quinobenzoxazine photocleavage reaction comigrate under gel electrophoresis (lane 5, Figure 7) with the 3′-phosphoglycolate termini products (*30*) from the bleomycin-Fe(II) cleavage reaction (lane 10, and see the enlarged section at the right panel in Figure 7). These results suggest that both 3′-phosphate and 3′-phosphoglycolate termini products are produced by the (*S*)-A-62176 photocleavage of DNA.

To further study the nature of the (*S*)-A-62176 DNA photocleavage products, the effect of alkaline treatment on the amount and mobility of the photoproducts was examined. After photocleavage, the labeled DNA was treated with NaOH (lane 8, Figure 7) or piperidine (lanes 6−11 of Figure 6B and lane 7 of Figure 7) and the products resolved by electrophoresis. As in the case prior to base treatment, the photoproducts after base treatment afford doublets of bands at each cleaved DNA site; however, after base treatment the slower migrating band of each doublet is much more intense, indicating the presence in the untreated photoproduct of DNA lesions that lead to 3′-phosphate termini cleavage products upon alkaline treatment. On the other hand, the intensity of the faster moving bands of each doublet shows either decreased intensity or little change after base treatment when compared to the bands produced by the photoproduct prior to base treatment, depending upon the particular cleavage site.

Gel electrophoresis of the products of photochemical DNA cleavage of 3′-labeled oligonucleotides by (*S*)-A-62176 was performed in order to investigate the nature of 5′-termini produced by photocleavage (Figure 8). In contrast to the doublet of bands observed at each DNA cleavage site when photocleavage was carried out with the 5′-end-labeled oligomer, only one band at each cleaved DNA base site is observed in the gel of the reaction of 3′-labeled oligonucleotides (lane 3), and each of these bands comigrates with the corresponding 5′-phosphate terminated Maxam−Gilbert sequencing products (lanes AG and TC).

In contrast to (*S*)-A-62176, the methylene blue-mediated photocleavage of DNA is quite inefficient prior to piperidine treatment (lane 5 in Figure 6A), while after piperidine treatment, DNA scission is clearly evident at every guanine site. The bands from the piperidine-treated methylene blue photocleavage reactions comigrate with the 3′-phosphate termini products (lane 5 in Figure 6B) from the Maxam−Gilbert sequencing reactions.

(S)-A-62176 cleaves DNA with moderate sequence selectivity at certain thymine and guanine residues, and the cleavage is more frequent in regions that are protected from DNase I digestion in the presence of (S)-A-62176. A synthetic

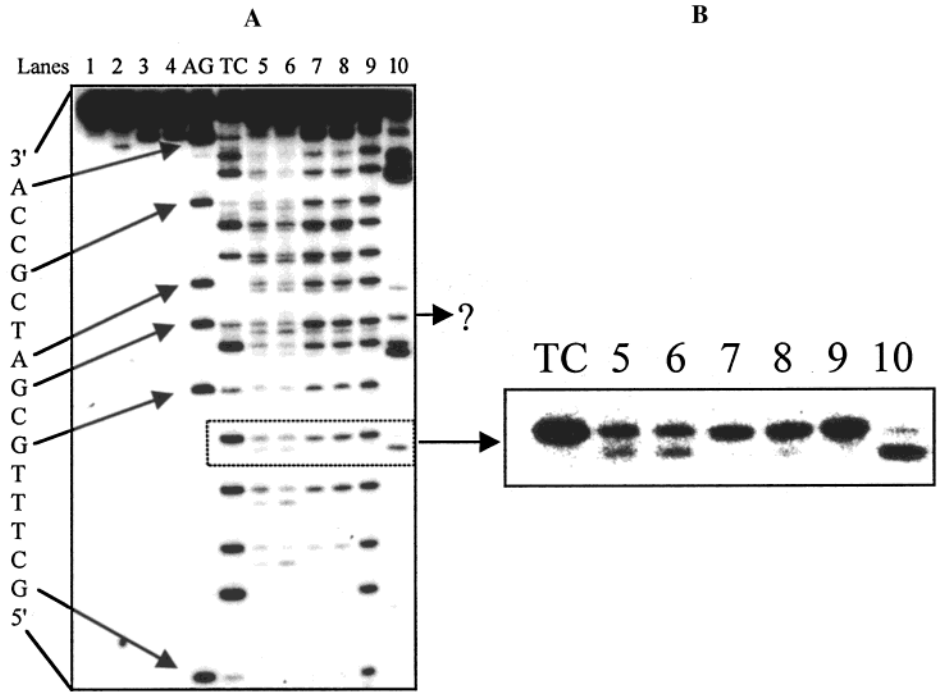

FIGURE 7: Comparison of (*S*)-A-62176 photocleavage with bleomycin cleavage. (A) Autoradiogram of 20% denaturing polyacrylamide gel of 5′-end labeled 18-mer DNA showing the DNA cleavage patterns. (B) Enlarged and overexposed portion of panel A. Lanes AG and TC contain the Maxam−Gilbert sequencing reaction products. Lane 5, oligonucleotide (2 μM) irradiated in the presence of 5 μM of (*S*)-A-62176. Lane 6−8, same reaction as that in lane 5 followed by NaBH4 treatment (lane 6), piperidine treatment (lane 7), and NaOH treatment (lane 8), respectively. Lanes 1−4, reactions corresponding to lanes 5−8 but without (*S*)-A-62176. Lane 9, hydroxyl radical cleavage reaction. Lane 10, bleomycin cleavage reaction.. [There is an unidentified band (indicated by question mark) in the bleomycin cleavage lane that does not line up with any of the 3′-phosphoglycolic acid or 3′-phosphate products. Further attempts to identify this product were unsuccessful.]

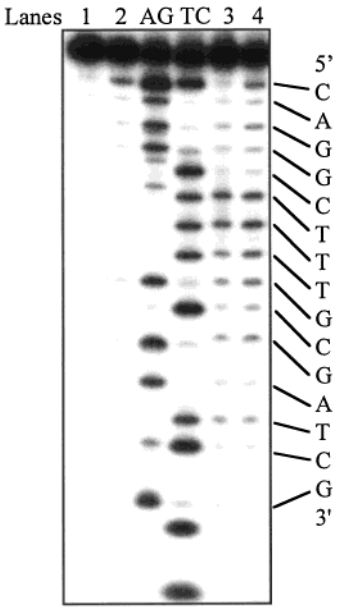

FIGURE 8: Photocleavage of the 3′-end labeled 18-mer DNA (3 μM in base pairs) by (*S*)-A-62176 (5 μM). Lane 1 and 2 are control DNA without and with heat-piperidine treatment, respectively. Lane AG and TC contain the Maxam−Gilbert sequencing reaction products. Lane 3 and 4 contain 5 μM of (*S*)-A-62176 without and with heat-piperidine treatment, respectively.

77-mer DNA was used to study the base selectivity of the photocleavage of DNA by (*S*)-A-62176. Figure 9 shows the gel electrophoresis of the photocleavage products along with the products of separate DNase I footprinting reactions on the same label 77-mer substrate. Although quinobenzoxazinze-mediated DNA photocleavage is observed at almost every DNA site, there are several preferred cleavage sites corresponding to certain guanine and thymine residues, as revealed in the histogram shown in Figure 10. Not every thymine is cleaved extensively by (*S*)-A-62176; TTTT or TTTTT tracts show weak cleavage. This result agrees with the previous drug binding studies indicating that the quinobenzoxazines prefer GC regions to A-tracts (*11*). A parallel experiment using a labeled 196 bp restriction enzyme fragment from the plasmid pBR322 also shows similar guanine and thymine base selective (*S*)-A-62176-mediated photocleavage pattern (data not shown). Therefore, the photocleavage of DNA by (*S*)-A-62176 has moderate sequence selectivity at certain guanine and thymine residues. The DNase I footprinting results demonstrate that the regions protected from DNase I digestion (sequence underlined in Figure 10) were extensively photocleaved by (*S*)-A-62176, showing a good correlation between the drug binding sites and the photocleavage sites.

DISCUSSION

Photochemical cleavage of DNA by fluoroquinolones has been investigated as a possible mechanism of the well-established phototoxicity of these drugs (*21*). The quinobenzoxazines are fluoroquinolone analogues that have previously been shown to undergo photochemical reaction to produce an unidentified, highly fluorescent photoproduct. This photochemical reaction of the quinobenzoxazines is dependent upon the formation of 2:2 quinobenzoxazine−Mg^{2+} dimers and is greatly facilitated in the presence of double-stranded DNA (*15*). Here we show that like certain fluoroquinolones, the quinobenzoxazine (*S*)-A-62176 can effect the photochemical cleavage of DNA.

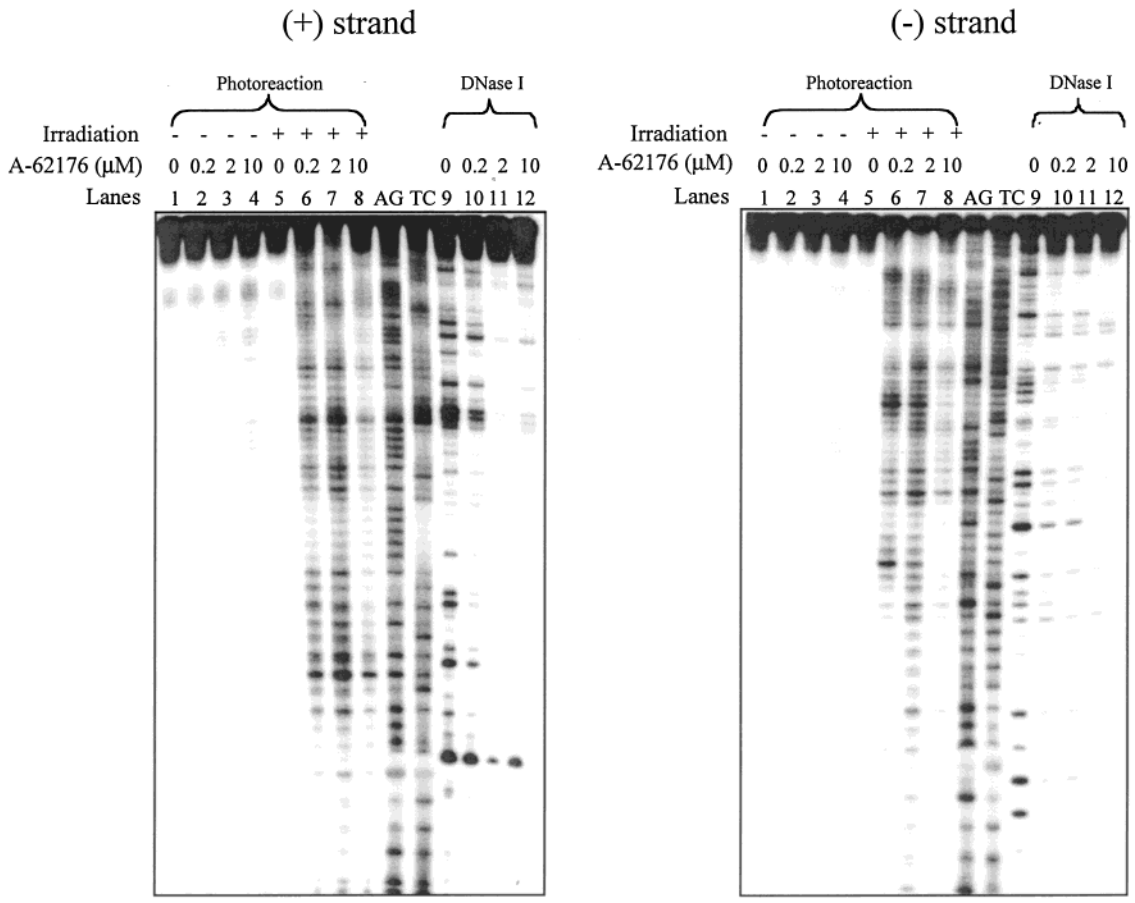

FIGURE 9: Comparison of the (*S*)-A-62176 photocleavage and DNase I footprinting of (*S*)-A-62176 DNA binding sites on the 5′-end-labeled 77-mer DNA (0.2 μM in base pairs). DNA photocleavage reactions were carried out at the indicated concentrations of (*S*)-A-62176 as in Figure 6 and followed by piperidine treatment. DNase I footprinting reactions were carried out in the presence of the indicated amount of (*S*)-A-62176 as described in the Materials and Methods. The DNA products were subjected to 12% denaturing polyacrylamide gel electrophoresis and autoradiography.

The photochemical DNA cleavage efficiency of (*S*)-A-62176 is much higher than the fluoroquinolones such as norfloxacin, ciprofloxacin, and enoxacin (Figure 2). Like the photochemical cleavage reported for the fluoroquinolones (*21*−*24*), the photocleavage by (*S*)-A-62176 affords frank, single-strand DNA breaks. The increased photocleavage efficiency of the quinobenzoxazine relative to the fluoroquinolones may be due to the difference in DNA binding between these two compounds: the fluoroquinolones do not bind to duplex DNA (*12*, *13*, *31*), while (*S*)-A-62176 binds double stranded DNA tightly by a magnesium-dependent intercalation interaction. In addition, the quinobenzoxazine chromophore may be better able to effect DNA cleavage when compared to the abbreviated fluoroquinolone chromophore. While the relative efficiency of the photochemical cleavage due to the quinobenzoxazine (*S*)-A-62176 would indicate that phototoxicity may be an issue with this potential anticancer agent, this photocleavage reaction might be beneficially employed in the photochemical mapping of drug−DNA binding sites in vitro (*5*) and in vivo.

The presence of Mg^{2+} is vital for the specific intercalation complex formation between (*S*)-A-62176 and DNA (*11*). In the absence of Mg^{2+}, the photocleavage efficiency of (*S*)-A-62176 is at least an order of magnitude less than in the presence of Mg^{2+} (Figure 1B and Figure 6A). The 5-descarboxy derivative of (*S*)-A-62176, which lacks the β-ketoacid unit that is vital for Mg^{2+} coordination and specific intercalation complex formation with duplex DNA, photocleaves supercoiled phage DNA with an efficiency 2 orders of magnitude less than that of (*S*)-A-62176 (Figure 3). The comparison of the DNase I footprint pattern due to the (*S*)-A-62176-Mg^{2+} complex and the (*S*)-A-62176 DNA photocleavage pattern in Figure 9 also suggests that DNA binding is important for the quinobenzoxazine-induced DNA photocleavage. Regions of DNA that are protected from DNase I digestion by (*S*)-A-62176 also undergo more extensive photocleavage.

To investigate the nature of the photochemical reactions leading to DNA strand scission by (*S*)-A-62176 a comparison of the effect of potential inhibitors of the photocleavage reaction on the fluorescence of the DNA-bound (*S*)-A-62176-Mg^{2+} dimer and on the previously reported DNA-facilitated photochemical degradation of (*S*)-A-62176 was undertaken. Fluorescence of the DNA-bound (*S*)-A-62176 is quenched by KI. KI is a widely used fluorescence quencher and is believed to operate by a combination of electron transfer and the so-called "heavy atom" effect (*32*, *33*). However, as Suh and Chaires have demonstrated (*34*), KI is unable to quench the fluorescence of either DNA-intercalated ethidium or DNA-minor groove bound Hoechst 33258. The inability of KI to quench these DNA-bound species has been attributed to the electrostatic repulsion between the iodide anion and polyanionic DNA, which prevents productive quenching encounters between the iodide and the excited state of ligands

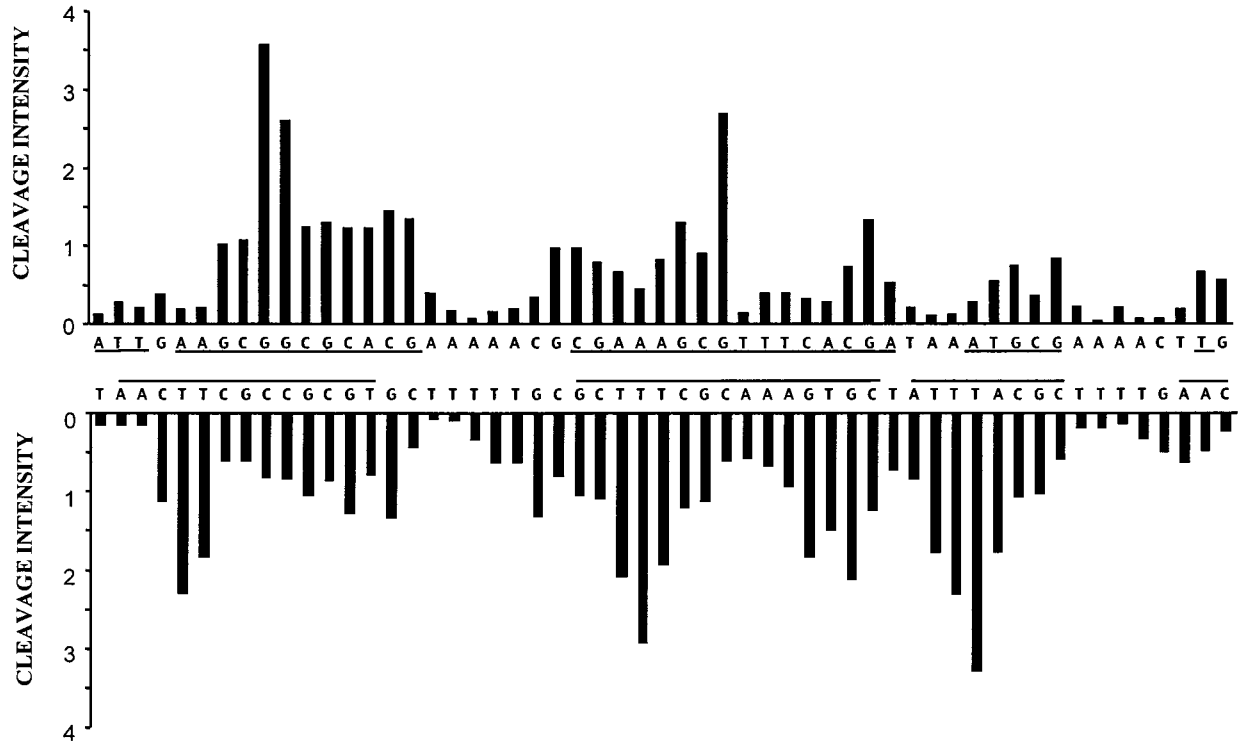

FIGURE 10: Comparison of the (*S*)-A-62176 photocleavage and DNase I footprinting of (*S*)-A-62176 DNA binding sites on the 5′-end-labeled 77-mer DNA. The intensity of the photocleavage reactions products (lanes 6 and 10 from Figure 9) for both strands were determined by densitometric scanning and are shown as histograms. The underlined sequences represent the regions protected from the DNase I digestion in the presence of (*S*)-A-62176.

closely associated with the DNA. The ability of KI to quench the fluorescence of DNA-bound (*S*)-A-62176 indicates that in the DNA−quinobenzoxazine complex the quinobenzoxazine chromophore is accessible to iodide anion. This observation is consistent with the previously reported model for how the quinobenzoxazines, typified by (*S*)-A-62176, bind to DNA. The quinobenzoxazines bind DNA as 2:2 quinobenzoxazine−Mg^{2+} dimers where one drug molecule of the dimer intercalates between DNA base pairs and the other is externally bound (*11*). Apparently, the more accessible externally bound quinobenzoxazine is available for fluorescence quenching by KI. DTT also quenches the fluorescence of the DNA-bound quinobenzoxazine by an undetermined mechanism.

In contrast to the fluorescence of DNA-bound (*S*)-A-62176, the DNA-facilitated production of the fluorescent photoproduct from (*S*)-A-62176 is very sensitive to a number of inhibitors, including DTT, KI, and, somewhat less, NaN_3. This indicates the intermediacy of a relatively longed-lived species in this photodecomposition pathway. The photochemical DNA cleavage reaction of (*S*)-A-62176 is inhibited by KI and only weakly by thiourea, DTT, and NaN_3. In the presence of concentrations of inhibitors sufficient to completely inhibit the production of the (*S*)-A-62176-derived fluorescent photoproduct, the photochemical cleavage of DNA is unaffected. This may indicate that these two photochemical reactions involve two distinct manifolds. Alternatively, photocleavage and production of fluorescent quinobenzoxazine-derived photoproduct may arise from two distinct intermediates (i.e., a DNA-centered radical cation and a quinobenzoxazine radical anion) of different accessibility to quenching agents along a common photochemical pathway. Photocleavage inhibition by KI at concentrations lower than those required to quench fluorescence indicates that cleavage does not occur directly from the quinobenzoxazine singlet state, but rather involves a longer-lived intermediate that is intercepted by iodide. A shorter-lived or less accessible DNA-centered intermediate may be formed from the interaction of the quinobenzoxazine excited state with the bound DNA. This DNA intermediate in turn gives rise to the observed DNA photocleavage products.

Photocleavage reactions involving 5′- and 3′-end labeled oligonucleotides reveal the complexity of the DNA cleavage process. At each DNA cleavage site up to four DNA photocleavage products are produced: the frank strand breakage products terminated with 3′-phosphate, 3′-glycophosphate, and 5′-phosphate, and a base-labile site. In addition to the overall coincidence of quinobenzoxazine DNA binding sites and DNA photocleavage sites, there is a slight sequence preference for the photochemical DNA cleavage reaction of (*S*)-A-62176 at guanine and thymidine residues. Although there is insufficient data as yet to speculate as to the exact nature of the photochemical reactions leading to DNA strand scission, the complexity of the process, and especially the identification of 3′-phosphoglycolate products, indicates that free radicals are involved. The involvement of free radicals during DNA cleavage is supported by the inhibition of the photocleavage in the presence of free radical scavengers such as NaN_3, DTT and thiourea. In addition, the 3′-phosphoglycolate products, formed by abstraction of the 4′-hydrogen (*35*, *36*), are strongly suggestive of a free-radical photochemical cleavage pathway. The base-labile DNA lesions that are produced may also arise via a free radical pathway. Abstraction of the H1′ hydrogen is known to result in the formation of deoxyribonolactone lesions that afford 3′-phosphate teminus strand breakage products upon

base treatment (*37*). An alternative pathway for the formation of base-labile sites, photoactivated base damage, seems less likely in light of the nearly equal formation of these lesions at T and G residues. Both H4′ and H1′ hydrogen atom abstraction indicate that the photochemical cleavage reaction occurs in the minor groove of DNA. Although the photochemical cleavage of DNA by (*S*)-A-62176 is oxygen dependent, it does not involve singlet oxygen or superoxide. Methylene blue-sensitized formation of singlet oxygen causes DNA depurination exclusively at guanine sites, these abasic sites undergo cleavage upon base treatment (*25*, *38*−*40*). Under our experimental conditions, methylene blue photosensitization indeed affords no frank strand scission and cleaves only the guanine sites of the 26-mer DNA after piperidine treatment (Figure 6B, lane 5). In contrast, the photocleavage by (*S*)-A-62176 affords frank strand scission at many sites, with moderate selectivity at certain guanine and thymine sites. Also, the singlet oxygen scavenger 2,2,6,6-tetramethylpyrrole does not inhibit the photocleavage (data not shown). Therefore, singlet oxygen is not likely the major source of DNA cleavage induced by (*S*)-A-62176. Similarly, superoxide or peroxide are not likely the source of free radicals because superoxide dismutase and catalase do not interfere with the photocleavage. Therefore, the most probable involvement of oxygen involves trapping of the carbon centered sugar radicals produced by hydrogen abstraction; further reactions of the oxygen-intercepted radicals lead to DNA cleavage products as demonstrated in many other cases (*35*, *36*, *41*−*44*).

In conclusion, the photochemical cleavage of DNA by the quinobenzoxazine (*S*)-A-62176 in the presence of Mg^{2+} is an exceptionally efficient process when compared to other fluoroquinolone analogues. The Mg^{2+} dependency of this photocleavage reaction and the overall coincidence of photocleavage sites with DNA binding sites indicates that the photocleavage proceeds from the previously reported quinobenzoxazine−Mg^{2+}-DNA complex. Mechanistic studies of this photochemical DNA cleavage reaction provide further evidence for the existence of two functionally distinct quinobenzoxazine molecules in this ternary complex, and serve to locate the complex in the minor groove of the DNA.

REFERENCES

1. Chu, D. T. W., and Maleczka, R. E. J. (1987) *J. Heterocycl. Chem. 24*, 453−456.
2. Chu, D. T. W., Hallas, R., Clement, J. J., Alder, L., McDonold, E., and Platter, J. J. (1992) *Drug Exp. Clin. Res. 18*, 275−282
3. Clement, J. J., Burres, N., Jarvis, K., Chu, D. T. W., Swiniarski, J., and Adler, J. (1995) *Cancer Res. 55*, 830−835.
4. Permana, P. A., Snapka, R. M., Shen, L. L., Chu, D. T. W., Clement, J. J., and Platter, J. J. (1994) *Biochemistry 33*, 11333−11339.
5. Kwok, Y., Zeng, Q., and Hurley, L. H. (1999) *J. Biol. Chem. 274*, 17226−17235.
6. Maxwell, A. (1992) *J. Antimicrob. Chemother. 30*, 409−414.
7. Mitscher, L. A., and Shen, L. L. (1992) in *Nucleic Acid Targeted Drug Design*, (Propst, C. L., and Perun, T. J. Ed.), pp 423−473, Marcel Dekker, Inc., New York.
8. Khodursky, A. B., and Cozzarelli, N. R. (1998) *J. Biol. Chem. 273*, 27668−27677.
9. Drlica, K., and Zhao, X. (1997) *Microbiol. Mol. Biol. Rev. 61*, 377−392.
10. Drlica, K. (1999) *Curr. Opin. Microbiol. 2*, 504−508.
11. Fan, J.-Y., Sun, D., Yu, H., Kerwin, S. M., and Hurley, L. H. (1995) *J. Med. Chem. 38*, 408−424.
12. Shen, L. L., Baranowski, J., and Pernet, A. G. (1989) *Biochemistry 28*, 3879−3885.
13. Shen, L. L., Mitscher, L. A., Sharma, P. N., O'Donnell, T. J., Chu, D. T. W., Cooper, C. S., Rosen, T., and Pernet, A. G. (1989) *Biochemistry 28*, 3886−3894.
14. Khac, S. B.-P., and Moreau, N. J. (1994) *J. Chromatogr. A. 668*, 241−247.
15. Yu, H., Hurley, L. H., and Kerwin, S. M. (1996) *J. Am. Chem. Soc. 118*, 7040−7048.
16. Christ, W., Lehnert, T., and Ulbrich, B. (1988) *Rev. Infect. Dis. 10* (Suppl. 1), 141−145.
17. Ferguson, J., and Johnson, B. E. (1993) *Brit. J. Dermatol. 128*, 285−295.
18. Halkins, H. (1988) *Rev. Infect. Dis. 10* (Suppl. 1), 258−262.
19. Wainwright, N. J., Collins, P., and Ferguson, J. (1993) *Drug Safety 9*, 437−440.
20. Rosen, J. E., Prahalad, A. K., Schlüter, G., Chen, D., and Williams, G. M. (1997) *Photochem. Photobiol. 65*, 990−996.
21. Iwamoto, Y., Kurita, A., Shimizu, T., Masuzawa, T., Uno, K., Yagi, M., Kitagawa, T., Oku, T., and Yanagihara, Y. (1994) *Biol. Pharm. Bull. 17*, 654−657.
22. Sortino, S., Condorelli, G., De Guidi, G., and Giuffrida, S. (1998) *Photochem. Photobiol. 68*, 652−659
23. Reavy, H. J., Traynor, N. J., and Gibbs, N. K. (1997) *Photochem. Photobiol. 66*, 368−373.
24. Martinez, L., and Chignell, C. F. (1998) *J. Photochem. Photobiol. B 45*, 51−59.
25. Specht, K. G. (1994) *Photochem. Photobiol. 59*, 506−514.
26. Kappen, L. S., and Goldberg, I. H. (1983) *Biochemistry 22*, 4872−4878.
27. Maxam, A. M., and Gilbert, W. (1980) *Methods. Enzymol.* 65, 499−560
28. Hertzberg, R. P., and Dervan, P. B. (1984) *Biochemistry 23*, 3934−3945
29. Sitlani, A., Long, E. C., Pyle, A. M. and Barton, J. K. (1992) *J. Am. Chem. Soc. 114*, 2303−2312.
30. Stubbe, J. and Kozarich, J. W. (1987) *Chem. Rev. 87*, 1107−1136.
31. Sissi, C., Andreolli, M., Cecchetti, V., Fravolini, A., Gatto, B., and Palumbo, M. (1998) *Bioorg. Med. Chem. 6*, 1555−1561.
32. Mac, M., Najbar, J., Phillips, D. and Smith, T. A. (1992) *J. Chem. Soc., Faraday Trans. 88*, 3001−3005.
33. Miller, J. C., Meek, J. S., and Strickler, S. J. (1977) *J. Am. Chem. Soc. 99*, 8175−8179.
34. Suh, D., and Chaires, J. B. (1995) *Bioorg. Med. Chem. 3*, 723−728
35. Giese, B., Beyrich-Graf, X., Erdmann, P., Petretta, M., and Schwitter, U. (1995) *Chem. Biol. 2*, 367−375.
36. Matsuura, T. (1987) in *The Role of Oxygen in Chemistry and Biology*(Ando, W., and Moro-oka, Y., Eds.) Vol. 33, Elsevier Science Publishers B. V., Amsterdam.
37. Greenberg, M. M. (1998) *Chem. Res. Toxicol. 11*, 1235−1248.
38. Sies, H. (1993) *Mutat. Res. 299*, 183−191.
39. Van den Akker, E., Lutgerink, J. T., Lafleur, V. M., Joenje, H., and Retel, J. (1994) *Mutat. Res. 309*, 45−52.
40. Joshi, R. R., Likhite, S. M., Kumar, R. K., and Ganesh, K. N. (1994) *Biochim. Biophys. Acta 1199*, 285−292.
41. Morin, B., and Cadet, J. (1995) *J. Am. Chem. Soc. 117*, 12408−12415.
42. O'Neill, P., and Fielden, M. (1993) *Adv. Radiat. Biol. 17*, 53−119.
43. Steenken, S. (1989) *Chem. Rev. 89*, 503−520.

BI001103X